



Cardiac support device (ASD) delivers bone marrow stem cells repetitively to epicardium has promising curative effects in advanced heart failure

Shizhong Yue^{1,2} · Muhammad Naveed¹ · Wang Gang¹ · Dingding Chen¹ · Zhijie Wang² · Feng Yu¹ · Xiaohui Zhou^{1,3,4} 

© Springer Science+Business Media, LLC, part of Springer Nature 2018

Abstract

Ventricular restraint therapy is a non-transplant surgical option for the management of advanced heart failure (HF). To augment the therapeutic applications, it is hypothesized that ASD shows remarkable capabilities not only in delivering stem cells but also in dilated ventricles. Male SD rats were divided into four groups ($n=6$): normal, HF, HF + ASD, and HF + ASD-BMSCs respectively. HF was developed by left anterior descending (LAD) coronary artery ligation in all groups except normal group. Post-infarcted electrocardiography (ECG) and brain natriuretic peptide (BNP) showed abnormal heart function in all model groups and HF + ASD-BMSCs group showed significant improvement as compared to other HF, HF + ASD groups on day 30. Masson's trichrome staining was used to study the histology, and a large blue fibrotic area has been observed in HF and HF + ASD groups and quantification of fibrosis was assessed. ASD-treated rats showed normal heart rhythm, demonstrated by smooth -ST and asymmetrical T-wave. The mechanical function of the heart such as left ventricular systolic pressure (LVSP), left ventricular end-diastolic pressure (LVEDP) and heart rate was brought to normal when treated with ASD-BMSCs. This effect was more prominent than that of ASD therapy alone. In comparison to HF group, the SD rats in HF + ASD-BMSCs group showed a significant decline in BNP levels. So ASD can deliver BMSCs to the cardiomyocytes successfully and broaden the therapeutic efficacy, in comparison to the restraint device alone. An effective methodology to manage the end-stage HF has been proved.

Keywords Heart failure · Myocardial remodeling; Bone marrow stem cells · ASD device · Cardiac support device · Ventricular restraint therapy

✉ Dingding Chen
chdd9968@aliyun.com

✉ Zhijie Wang
wangzj@semi.ac.cn

✉ Feng Yu
yufengcpu@163.com

✉ Xiaohui Zhou
zhxh@cpu.edu.cn

¹ Department of Clinical Pharmacy, School of Basic Medicine and Clinical Pharmacy, China Pharmaceutical University, School of Pharmacy, Nanjing, Jiangsu Province 211198, People's Republic of China

² Key Laboratory of Semiconductor Materials Science, Institute of Semiconductors, Chinese Academy of Sciences, Beijing 100083, People's Republic of China

³ Department of Surgery, Nanjing Shuiximen Hospital, Nanjing, Jiangsu Province 210017, People's Republic of China

⁴ Department of Cardiothoracic Surgery, Zhongda Hospital affiliated to Southeast University, Nanjing, Jiangsu Province 210017, People's Republic of China

1 Introduction

HF is a common and complex disease condition in the cardiovascular system (CVS), which leads to various complex symptoms and ultimate death (Francis 1988; Cotter et al. 2010; Gullestad et al. 2012). It is characterized by structural or functional cardiac abnormalities and causes the impair filling of ventricles ultimately, leading to imbalance energy demand between heart and body, as well as, several complications (Alskaf et al. 2016). Although in the past few decades, clinical research regarding the diagnosis, prevention, and management of HF has progressed impressively however, HF is still a primary cause of death in developed countries with a worldwide prevalence of 20 million, and its occurrence is estimated to increase in parallel with the aging population (Sung and Dyck 2015; Danilowicz-Szymanowicz et al. 2016). Up gradation of pharmacological therapies for HF is taking place rapidly and has been actualized according to the American (Yancy et al. 2013; Kawasaki et al. 2012) and

European (Miro et al. 2016) HF guidelines. In particular, device interventional therapies for the management of HF at various stages are also under active investigation and significant advancement has been made in the recent years. Currently, there are several approved therapies which are being used for the management of HF at various stages, however, these therapies lead to reserved symptom relief for congestive heart failure (CHF) but are incapable to recover long-term survival outcomes significantly, except heart transplantation (Andrew and Macdonald 2015). Whereas, genetic variations, tissue mismatching, differences in certain immune response and socioeconomic crisis are some major concern with cardiac transplantation, suggested an alternate bridge to transplant (BTT) or destination therapies (DT).

The ventricle reconstruction therapy was developed in the last two decades by Acorn CorCap. It is a non-transplant surgical VRT, wherein the overall goal is to wrap the dilated, failing heart with prosthetic material to automatically constrain the heart at end-diastole, stop further remodeling, and thereby ultimately improves patient symptoms, ventricular function, and survival outcomes (Koomalsingh et al. 2013). Up till now 3 premature ventricular restraint devices (Naveed et al. 2018) i.e. Acorn CorCap Cardiac Support Device (CSD) (Wenk et al. 2013; Kubota et al. 2014), Paracor Heart Net device (Oliveira et al. 2014; Atluri and Acker 2013) has undergone human trial and Quantitative Ventricular Restraint (QVR) device (Ghanta et al. 2007; Magovern 2005) studies in animals has been developed. In fact, neither a pharmacological interventions nor mechanical device implantation as a single therapy can meet the demand of the advanced HF patients.

Until now, no attention has been given to the epicardium role in heart regeneration, but the relevant investigation suggests that like embryonic stage development, the contraction and relaxation properties of the heart have a signaling center for the heart regeneration (Limana et al. 2011). However, the use of stem cells holds an important pledge (Yancy et al. 2013; Geft et al. 2008) and emerges as an alternate for transplantation (Ishida et al. 2015). Currently, there are various types of stem cells delivered to the heart by different ways (Sheng et al. 2013) in the past decades. Although, it was realized that neither skeletal myoblasts nor embryonic stem cells would become the cells of choice, and there is concern that pluripotent stem cells might prove to be tumorigenic (Sanganalmath and Bolli 2013a). However, the autologous bone marrow-derived progenitor cells (stem cells) are shown to be of promise (Fernandez-Ruiz 2016; Fisher et al. 2013). The utilization of BMSCs not only minimizes the time but also reduces the cost of therapy (Michler 2014; Yu et al. 2010). Transplantation of adult BMSCs can improve LV function and reduces infarct size, so it tumbles the incidence of death, stent thrombosis, and recurrent MI in patients (Jeevanantham et al. 2012).

Therefore, the method for delivering BMSCs is a vital milestone and has been investigated for years (Rasmussen et al. 2011). The delivery of stem cells could be conducted through cell-seeded matrix onto the epicardial surface (Bilgimol et al. 2015) and hydrogel poses beneficial for injectable scaffold (Cheng et al. 2012). In addition, the delivery of cells could also be carried out through VRDs and multi-center trials conducted through LVAD for delivery of cells, which appeared to be safe and efficient (Lok et al. 2015; Ascheim et al. 2014). Another study of stem cells was directed with restraint device, demonstrates that a combined therapy of VRD and stem cells offers superior potential for improving diastolic and systolic function, reducing adverse remodeling and fibrosis, over the conventional stem cell therapy and VRT (Shafy et al. 2013).

To obtain the optimum therapeutic benefit, VRD combining with stem cells is highly required, but up till now, no restraint therapy has been able to provide this dual effect in single action (Naveed et al. 2017). In this study, an ASD device was designed by using silicone, a highly biocompatible material (Jaganathan and Godin 2012; Bernik 2007). So ASD is able to provide cardiac support and its unique structure has also been able in delivering the stem cells to cardiomyocytes. It was demonstrated that VRT with such characteristics showed the superior therapeutic benefits to relieve HF symptoms over the restraint therapy alone.

2 Materials and methods

Male Sprague-Dawley (SD) rats (250–300 g) were purchased from College of Veterinary Medicine, Yangzhou University (License # SCXK (Su) 2015–2005, Yangzhou, China. Silk suture and 6.0 polypropylene sutures were brought from Shanghai Jinhuan Chemical Co., Ltd., Shanghai, China. Ventilator (HX-300S), BL-420 multi-channel physiological system and ECG were obtained from Chengdu technology & market Co., Ltd., Chengdu, China. The polyethylene catheter and implantable catheter were purchased from Jiangxi Hongda Medical Equipment Group Co., Ltd. Nanchang, Jiangxi, China. Biebrich scarlet-acid fuchsin kits and Trichrome's staining kit were purchased from Beyotime Institute of Biotechnology, Haimen, China. Rat BNP ELISA kit was purchased from Shanghai Jinma Biological Co., Ltd., Shanghai, China. This study was carried out according to strict and recommendations and Guidance of the Care and Use of Laboratory Animals of the National Institutes of Health. The protocol was approved by the Committee on the Ethics of Animal Experiments of the China Pharmaceutical University, School of Pharmacy. All surgery was performed under pentobarbital sodium anesthesia, and all efforts were made to minimize suffering.

2.1 Study design

A total of 24 male SD rats were randomly divided into 4 groups ($n = 6$): normal, HF, HF + ASD, HF + ASD-BMSCs respectively (Fig. 1). HF was induced by ligation of the left anterior descending (LAD) coronary artery ligation as previously described (Qiu et al. 2014). Prior to anesthesia, all the rats were shaved, weighed, disinfected and scrubbed from the neck and chest area with 75% ethanol and anesthetized by intraperitoneal injection of 3% Phenobarbital sodium (30 mg/kg). Anesthetized rats were laid in a supine position and endotracheal intubation was performed. Ventilation was made possible by connecting the endotracheal tube to HX-300S ventilator at a breathing rate of 80/min and tidal volume 10 mL. After stable breathing, the chest was opened between the 3rd and 4th intercostals space and a chest retractor was placed to depict the LV. Left coronary artery was recognized and then ligated with 6.0 polypropylene sutures to provoke HF, and confirmed by taking the ECG and BNP levels. Chest retractor was withdrawn and the ribs were rejoined together by discontinuing stitching. In case of treatment groups, first the device was implanted and then the chest was closed for further experiments.

2.2 Isolation of BMSCs

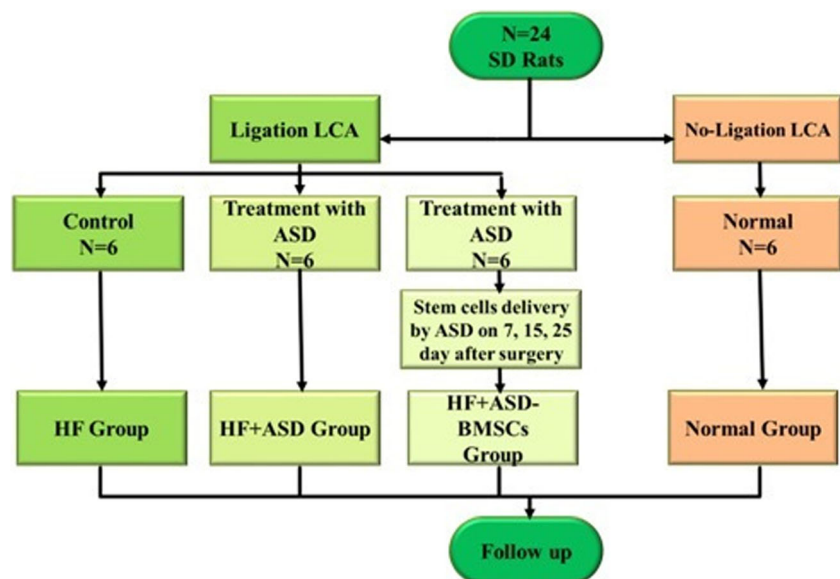
The rats were soaked in 75% ethanol for 10 min and euthanized. The tibias and femurs were bilaterally dissected to depict the epiphyseal plates under sterile conditions. An injector containing PBS was used to rinse out the bone marrow awaiting the bone cavity became white. Consequently, the rinsed bone marrow was blown and crashed into a cell suspension slowly. The suspension was centrifuged at 1500 rpm/

min for 25 min to gradient extraction BMSCs. A proper amount of Dulbecco's modified Eagle's medium was added to precipitate and the mixture was blown into a cell suspension and located into culture flasks to keep it as a reserve (Tian et al. 2014). For detection of rat mesenchymal BMSCs, rat surface antigen CD90, CD29, CD45 as a test indicator and fluorescently labeled antibodies like PE-CD90, APC-CD29, and FITC-CD45. F3 generation of BMSCs and trypsin digestion for 1 min plus 1 mL complete medium for termination of digestion was taken. The cells were centrifuged (1000r/5 min) and washed with PBS for cell count (1×10^6 cells/mL) repeatedly. The re-suspended cells were added to seven 1.5 mL EP tubes, each containing 500 cells. Like Blank control group +5 μ L PBS, PE-90 group +0.75 μ L PE-90, APC-29 group +6.25 μ L APC-29, FITC-45 group +2.5 μ L FITC-45, Test group +0.75 μ L PE-90 + 6.25 μ L APC-29 + 2.5 μ L FITC-45 and 2 Ibid Test groups then put into the refrigerator at 4 °C and dark incubation for 30 min. Washed twice with PBS and centrifuged (1000r/5 min). After centrifugation, PBS re-suspended each tube 300 μ L and filtered on the machine test. The positive rate of CD90 was 98.4%, the positive rate of CD45 was 1.29%, and the positive rate of CD29 was 98.8%.

2.3 ASD device

An active hydraulic ventricle supporting drug delivery system (ASD) consists of highly biocompatible silicon based (Zhou 2012; Naveed et al. 2017) fistulous net cover surrounding both the ventricles as shown in Fig. 2a. All the hollow tubes completely communicate with each other or form a plurality of independent areas, and the interior of each independent area is intercommunicating. The interconnecting tubules have

Fig. 1 Study design of experiments



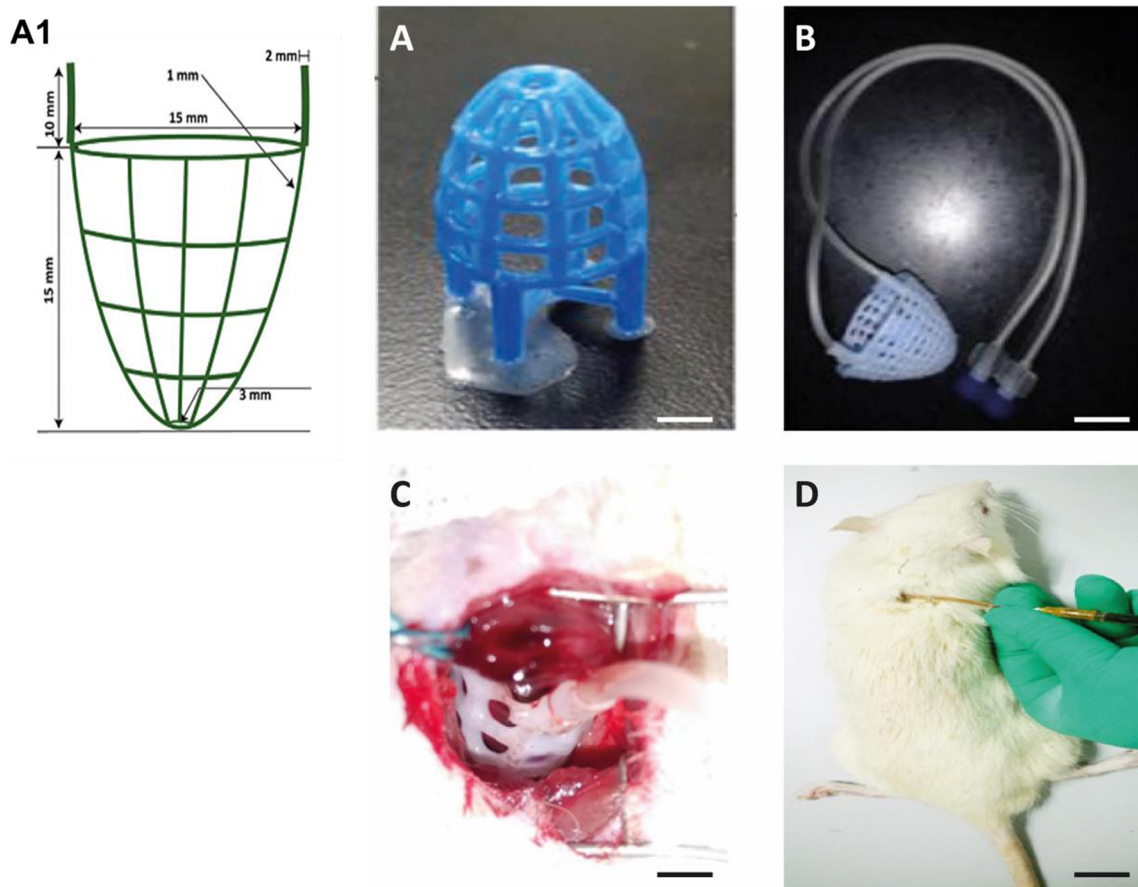


Fig. 2 (a1) Dimensions of ASD device in SD rats, (a) Silicon base ASD device, (b) ASD connected with implantable catheter, (c) ASD device implantation, (d) Catheter opening in the skin for BMSCs injection, scale bar 100 μm

some intentionally designed apertures at the internal surface, with the purpose to generate communications of materials or signals between the heart and the net cover. Then the net cover can be connected to an administrating system outside the body via the ends connected to the exterior of the body as in Fig. 2d. Using ASD device, BMSCs could be delivered by the fluid inside the tubes and it could directly affect cardiomyocytes (Ascheim et al. 2014), by producing direct biological action on cardiac muscle or other heart tissues without entering blood circulation. Variety of therapeutic materials can be filled from the outside, spread all around the net cover, and then applied to the ventricle via the apertures (Naveed et al. 2017). Diameter of the hollow tubules and apertures are most important in the smooth delivery of therapeutic agents. When the diameter of the apertures is not larger than half of the diameter of the hollow tube, the hollow tube performs best. And if the diameter of the apertures is too large, the effect of the hollow tubes will be reduced. Particularly, the diameter of the hollow tubes is 1–2 mm, wherein the diameter of the apertures is 0.5–1.0 mm. Tubes of diameter within this scope have good support effect on the heart wall, good hydraulic reactivity, and good permeation efficiency to the heart tissue for the medicine (Zhou 2012). The size of ASD device is different for different

animals; the size for SD rats has been shown in Fig. 2a1. Accordingly, the species, concentration, a dose of stem cells, and speed of administration can be well adjusted outside the body.

2.4 ASD device implantation

After the confirmation of HF, pericardium was exposed and the ASD device was placed around the heart ventricles, which was achieved by sliding the device over the epicardium, up to the level of the atrioventricular (AV) junction (Fig. 2c). After achieving the correct position on heart it was then stitched with AV junction by prolene sutures (4–0) (Fig. 2). (Starling and Jessup 2004). The ASD device was connected to an implantable catheter (Fig. 2b) and ASD portacath was tunneled subcutaneously through the second intercostals space into the left anterior chest wall and was extended outside the body through the 1 cm opening made in the skin at spinotrapezius as shown in Fig. 2d. Chest retractor was withdrawn and the ribs were rejoined together by discontinuous stitching. After the placement of the ASD device, rats were divided into 2 tentative groups ($n = 6$) namely HF + ASD and HF + ASD-BMSCs groups. Postoperatively, animals received penicillin

sodium for antibiotic prophylaxis (5 wU/100 g i/m every 24 h for 5 days).

2.5 BMSCs injection

After successful implantation of ASD device, the BMSCs 0.5 mL/kg.day (1 mL = 1×10^6) was injected into HF + ASD-BMSCs group on the 7th, 15th and 25th day, through an exterior opening from the ASD as shown in Fig. 2d.

2.6 Electrocardiography

Rates were sedated with 10% chloral hydrate and then detained in the supine position on the table and the ECG machine having four electrodes was inserted into the limbs of the rats subcutaneously. Briefly, a black electrode was inserted into the right lower limb, red into the right upper limb, green into the left leg and yellow into the left upper limb. Series of ECG was demonstrated in all rats at pre-infarction, post-infarction, on the 7th, 15th and 30th day of infraction.

2.7 Assessment of BNP levels

Brain natriuretic peptide (BNP) or B-type natriuretic peptide is the gold standard biomarker in the diagnosis and prognosis of HF. BNP serum concentration was determined by ELISA method using RAT BNP ELISA kit according to the manufacturer's instructions. The blood of rats was collected and centrifuged at 2000 rpm/min for 2 min at 4 °C, and the supernatant (blood plasma) was collected. The plasma samples were diluted with the ratio of 1:4 and a stop solution was added then the BNP was measured.

2.8 Hemodynamic parameters

After achieving the steady breath, the right carotid artery (RCA) was distally ligated through a longitudinal incision on the right side of the neck and fixed to prevent excessive bleeding. One end of polyethylene catheter was introduced into the LV through the RCA and the other end was linked with BL-420 multi-channel physiological signal system. At stable conditions of hemodynamic all parameters were considered at the end of study period namely, mean left ventricular end diastolic pressure (mLVEDP), mean left ventricular systolic pressure (mLVSP), $-dp/dt_{max}$ and dp/dt_{max} through the BL-420 multi-channel physiological system. Heart rate was also taken digitally through BL-420 multi-channel physiological signal system on preoperative, postoperative, 7th, 15th and 30 day and mean data was calculated at the end of the study period.

2.9 Histopathology

After 30 days all the rats were euthanized and muscle tissues were excised up to neck region from the xiphoid, and the chest plate was removed completely along the muscles and ribs to expose the heart. The aorta was fixed with silk suture to avoid excessive bleeding and the heart was harvested. The heart was perfused in PBS (1:100) to flush out any remaining blood and fixed in 10% formalin. The heart was sliced into 5 μ m coronal sections, dehydrated with ascending ethanol series (70, 80, 90, 95, 100%), and embedded in paraffin. Masson's trichrome staining was used to differentiate between collagen and muscle fibers. Trichrome staining was accomplished by applying Weigert iron hematoxylin followed by Biebrich scarlet-acid fuchsin (plasma stain), phosphomolybdic-phosphotungstic acid, and aniline blue (fiber stain) on 5 μ m sliced section of heart on the slides (Rüder et al. 2014). Images from the sections were captured digitally by using Image Manager Software. The degree of fibrosis was quantified by using ImageJ software 4.7.0.

2.10 Follow-up studies

Electrocardiographic data were collected at pre-operated, 25 min after ligation, 7th, 15th and 30th day after ligation, respectively. Similarly, BNP was examined at pre-operative, post-operative after 7th, 15th and 30th day for each model group. Hemodynamic studies were done on the 30th day of experiment. For histological examination the heart was excised and the images were developed from the heart tissue after Masson's trichrome staining.

2.11 Statistical analysis

The SPSS 19 statistical package was used to perform all statistical evaluations (SSPS Inc., Chicago, IL, USA). All data were summarized and displayed as mean value (SD) for the incessant variables as a number of rats plus the percentage in each group for categorical variables. The one-way Kolmogorov-Smirnov test was used to assess the distributions. Levels of late apoptotic cells could not be converted to normal distribution, thus the variables were categorized into tertiles. All the above analyses were considered significant at $P < 0.05$.

3 Results

3.1 Electrocardiography

Prior to any experimental procedure all rates displayed a normal electrocardiographic waveform, with discrete P waves, QRS complexes and T waves, as shown in Fig. 3(a, y, d).

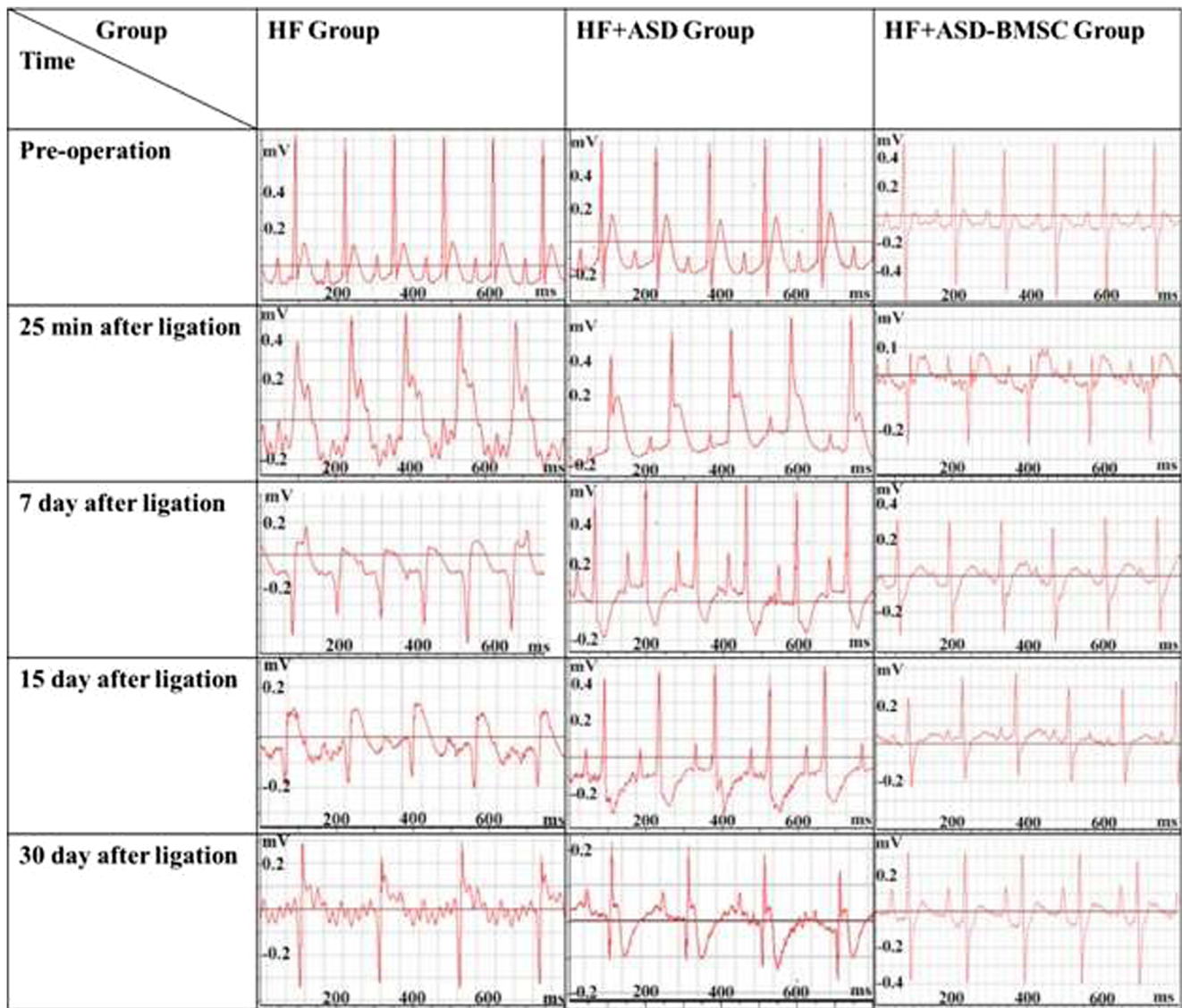


Fig. 3 Electrocardiogram (ECG) observations for preoperative, 25 min, 7th, 15th and 30th day after ligation of different treatment groups, HF, HF + ASD, HF + ASD-BMSC, $n = 3$

The ECG analysis showed noticeable abnormalities early after 25 min of HF induction, including QRS widening, ST elevation and PR interval prolongation, followed by the appearance of a peak known as ‘hyperacute T’ wave (Khan et al. 2007; Fazan et al. 2015) in HF group [Fig. 3e]. On the 7th and 15th day, the “T” wave became abnormal and pathological “Q” showed up on the 30th day, as demonstrated in Fig. 3(j, m, p). The elevated “ST” at 25 min was observed to be at declining level on the 7th and 15th day in HF + ASD group [Fig. 3(z, α , β)], and the ECG was illustrated to be normal on the 30th day in this group as shown in Fig. 3(μ). In HF + ASD-BMSCs group, in the initial 25 min, a pathological “Q” wave with decline was observed in Fig. 3(g). The “ST” wave also declining trend on the 7th and 15th day and a normal ECG was demonstrated at the end of study [Fig. 3(i,o,r)].

3.2 Histopathology

Masson’s trichrome staining showed that collagen fibers and fibrosis has been highlighted with blue coloration whereas the muscle fibers has been shown with red (Fig. 4a). In normal group a healthy myocardium is seen by red staining, while HF group presents a large amount of blue fibrotic tissue. The HF + ASD group also shows blue fibrotic but lesser than HF group while the HF + ASD-BMSCs group presents a fibrosis free image. In addition, the quantification of fibrosis by ImageJ software also showed similar observations (Fig. 4b).

3.3 Assessment of BNP levels

The BNP level in HF, HF + ASD and HF + ASD-BMSCs groups at preoperative, postoperative, after 7th, 15th and

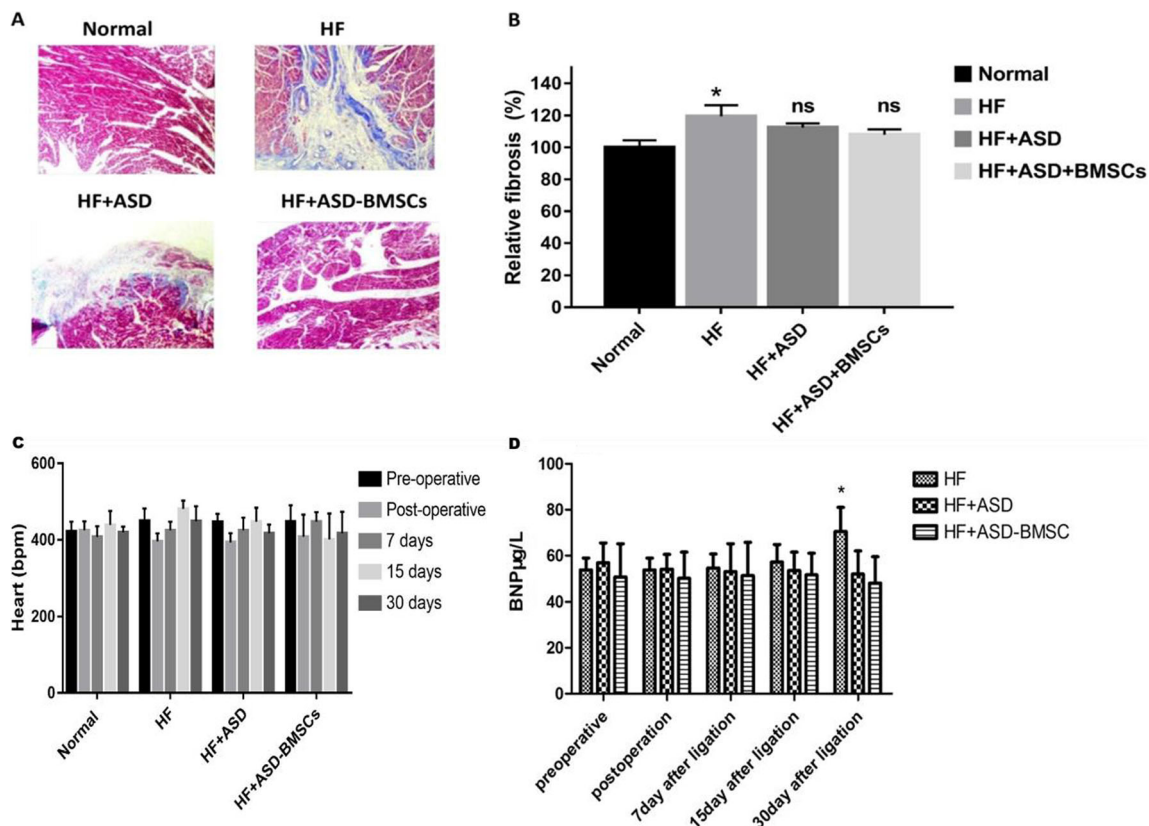


Fig. 4 Histopathology of heart tissues, (a) Masson's trichrome staining of cardiac tissue and fibrosis mark-up on digitized slides, (b) Quantification of fibrosis of heart tissues obtained from different treatment groups, $n = 3$,

(c) Heart rate and, (d) Plasma BNP level of preoperative, postoperative, 7th, 15th and 30th day of different treatment groups, ($P < 0.05$) HF vs HF + ASD and HF vs HF + ASD-BMSCs at 30 days, $n = 3$

30th day of ligation (Fig. 4d) and result showed that HF + ASD-BMSCs group showed a lower BNP level in blood (after ligation) compared to HF and supplementary treatment groups. The BNP values of HF + ASD-BMSC group at 30th day of ligation is significantly lower than that of pre-operative postoperative, 7th and 15th day after ligation.

3.4 Hemodynamic parameters

The LV hemodynamic parameters were calculated in all groups for assessment of ventricular performance as shown in Fig. 5. The diastolic parameter LVEDP in HF group is higher than normal, HF + ASD and HF + ASD-BMSCs groups. The HF + ASD-BMSCs group showed a decline tendency in LVEDP compared with the HF + ASD group. The LVSP tends to decline in HF group rather than in normal group, but HF + ASD and HF + ASD-BMSCs groups showed no significant difference with normal group. The cardiac contractility parameters (e.g., dp/dt_{max} decline and $-dp/dt_{max}$ incline) in HF group when compared with the others groups as shown in Fig. 5c, d. Heart rate of HF + ASD-BMSCs group was brought to normal as compared to supplementary treatment groups (Fig. 4c).

4 Discussion

Several mechanisms are shown to be related to the pathogenesis of HF such as cardiomyopathy, hypertension and coronary artery disease (CAD). Current therapies for HF management has improved symptoms and increased life expectancy, but the basic problem for tissue repair of cardiac damage is far from being resolved. Since the first publication on BMSCs in 2001 (Sanganalmath and Bolli 2013b; Vrtovec et al. 2013), a great deal of research interest has been focused on cells therapy as well as the clinical and preclinical applications. These studies revealed capability of the stem cells populations to improve cardiac function and attenuate adverse LV remodeling in both non-ischemic and ischemic cardiomyopathy (Vrtovec et al. 2013; Taylor and Robertson 2009). However, due to the absence of gap junction between the implanted cells and the host myocardium as well as the low survival possibility of the cells, recent studies suggest that the ventricle function is improved to a negligible level (Donndorf et al. 2011). To make this therapy more effective in a clinic, the issues like the correct dose, route of administration, and frequency of cell administration has to be addressed (Taylor and Robertson 2009). In particular, the

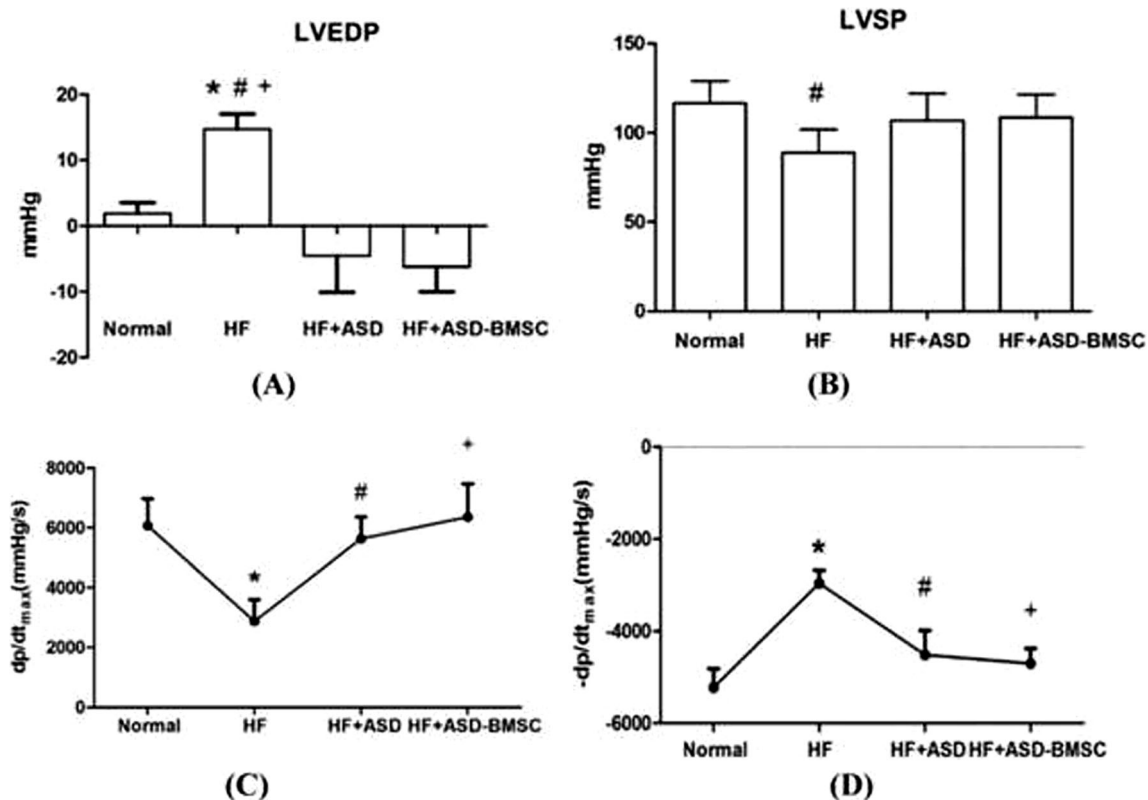


Fig. 5 Changes in the hemodynamic parameters of each group, (a) LVEDP ($*P < 0.05$) HF vs Normal, ($^{\#}P < 0.05$) HF + ASD vs HF and ($^{+}P < 0.05$) HF + ASD-BMSC vs HF, (b) LVSP ($*P < 0.05$) Normal vs

HF. Cardiac contractility (c) and (d) results are expressed as dp/dt_{max} and $-dp/dt_{max}$ ($*P < 0.05$) HF vs Normal group, ($^{\#}P < 0.05$) HF + ASD vs HF, and ($^{+}P < 0.05$) HF + ASD-BMSC vs HF

route and method of delivering cells, which determines the survival of transplanted cells, are of great importance (Smith et al. 2013).

Through extensive investigation, it has been demonstrated that ASD has two impressive benefits, by providing cardiac support to the heart and relieving the relevant symptoms, and showing the capacity to deliver stem cells. Consequently, the severity of HF could be greatly relieved and no renal dysfunction was observed. Indeed, the electrocardiography showed numerous abnormalities in HF (Fig. 3). The most frequently seen electrocardiographic abnormality is broad T-waves, small R-waves, deep Q-waves and ST-elevation, which is characteristic feature of dilated ventricular and MI (Chrastina et al. 2014). These abnormalities were observed in HF group on 7th, 15th and 30th-day, similarly it was noted in HF + ASD treated rats on 30th-day. While HF + ASD + BMSCs group showed improvement in treating dilated ventricle, ventricular relaxation and relieving HF symptoms. Which was characterized by smooth ST-segment, upright T-wave and normal Q-wave (Konopelski and Ufnal 2016; Dragojevic-Simic et al. 2004). Besides, ASD device was found safe and feasible regarding the electrical activity of the heart; furthermore, it improved cardiac performance and did not alter the structure and function of the myocardium.

To further confirm the morphological and functional changes, the molecular marker of HF at various time periods during the study was evaluated. The level of BNP increased with the development of HF after coronary artery ligation (Karlström et al. 2016) and successfully brought back to normal when treated with ASD-BMSCs (Fig. 4d). The level of BNP in HF + ASD-BMSCs group was found to be significantly lower than that of other model groups, revealing the effective delivery of stem cells by ASD and thus proving that the use of ASD with stem cells has a greater beneficial effect on HF than using restraint device alone. In addition, through the characterization of decreased LVSP and $-dp/dt_{max}$, amplified LVEDP, and extended dp/dt_{max} in HF + ASD-BMSCs group (Eleawa et al. 2015), demonstrated that both diastolic and systolic functions of heart in HF rats have been well impaired (Fig. 5). In this condition, the BMSCs delivered by ASD with an optimized therapeutic level has been identified to restore the physiology, maximize the reduction in mLVEDP throughout the cardiac cycle, decrease the area of infarction damage, improve mechanical efficiency and minimize the effects on systemic hemodynamic (Lavine et al. 2013).

Masson's trichrome staining is a valuable histopathologic tool and commonly used to differentiate collagen fibers from tissues and muscles (Fig. 4a). The acidophilic cytoplasm of myocardial tissues was stained with an

acidic dye. Collagen, a comparatively loose texture is easily penetrable by most dyes. However, after the following treatment, the dye will easily diffuse out, permitting collagen to be stained with aniline blue and will give a blue stained collagen fiber (Malatesta 2016). Cardiac cell death occurs after LAD coronary artery ligation (Bialik et al. 1997) and becomes noticeable in HF group on the 30th day. Left ventricular remodeling is categorized by hypertrophy and fibrotic changes (Travers et al. 2016) while death of cardiac cells leads to decrease in contractile force (Orogo and Gustafsson 2013). The histological examination by Masson's trichrome staining showed an apparent picture of all the groups. The HF group showed a high blue fibrotic area which confirms the successful induction of HF (Li et al. 2012). After the treatment with ASD-BMSCs, the group showed a large improvement when compared to HF + ASD and HF groups. The optimized ventricular restraint reverses the pathological LV dilation and stem cell therapy improves LV function (de Jong et al. 2013). This is attributed to the dual-effect of ASD device. To summarize, HF group showed both systolic and diastolic dysfunction. While HF-ASD + BMSCs leads to greater reduction in LV trans-myocardial pressure and ventricular wall stress, which leads to greater reverse remodeling as compared to HF + ASD group.

5 Conclusions

In summary, herein, for the first time, it has been proved that combination of VRD together with a biological stem cells-based regenerative approach turns out to be of great promise to the treatment of HF. The constructed therapeutic platform for the management of advanced HF exhibits multiple therapeutic functions in single action, by considering that multiple therapeutic materials, like stem cells, drugs, and diagnostic material could be delivered in a well-controlled way. Future efforts should be focused on equipping the ASD with more bi-directional biosensors to make the device more powerful, not only for the relevant disease treatment but also for the effective diagnosis.

Acknowledgments This work was supported by the National Found for Fostering Talents of Basic Science (NFFTBS), [grant number J1030830]. We are grateful to Dr. Michael Deininger (Medical innovation center, University of Michigan, USA) for his encouraging and supporting role for this research. We are highly thankful to Mr. Muhammad Karim Ahmed from CRI for critically reviewing the text of this paper.

Compliance with ethical standards

Conflict of interest All the authors declare that there is no conflict of interest. All the authors read and approved the manuscript.

References

- E. Alskaf, A. Tridente, A. Al-Mohammad, Tolvaptan for heart failure, systematic review and meta-analysis of trials. *J. Cardiovasc. Pharmacol.* **68**(3), 196–203 (2016)
- J. Andrew, P. Macdonald, Latest developments in heart transplantation: a review. *Clin. Ther.* **37**, 2234–2241 (2015)
- D.D. Ascheim, A.C. Gelijns, D. Goldstein, L.A. Moye, N. Smedira, S. Lee, C.T. Klodell, A. Szady, M.K. Parides, N.O. Jeffries, Mesenchymal precursor cells as adjunctive therapy in recipients of contemporary left ventricular assist devices. *Circulation* **129**, 2287 (2014)
- P. Atluri, M.A. Acker, Diastolic ventricular support with cardiac support devices: an alternative approach to prevent adverse ventricular remodeling. *Heart Fail. Rev.* **18**, 55–63 (2013)
- D.L. Bernik, Silicon based materials for drug delivery devices and implants. *Recent Pat. Nanotechnol.* **1**, 186 (2007)
- S. Bialik, D.L. Geenen, I.E. Sasson, R. Cheng, J.W. Horner, S.M. Evans, E.M. Lord, C.J. Koch, R.N. Kitsis, Myocyte apoptosis during acute myocardial infarction in the mouse localizes to hypoxic regions but occurs independently of p53. *J. Clin. Invest.* **100**, 1363–1372 (1997)
- J.C. Bilgimol, S. Ragupathi, L. Vengadassalopathy, N.S. Senthil, K. Selvakumar, M. Ganesan, S.R. Manjunath, Stem cells: an eventual treatment option for heart diseases. *World J. Stem Cells* **7**, 1118–1126 (2015)
- K. Cheng, A. Blusztajn, D. Shen, T.S. Li, B. Sun, G. Galang, T.I. Zarebinski, G.D. Prestwich, E. Marban, R.R. Smith, L. Marban, Functional performance of human cardiosphere-derived cells delivered in an in situ polymerizable hyaluronan-gelatin hydrogel. *Biomaterials* **33**, 5317–5324 (2012)
- A. Chrastina, P. Pokreisz, J.E. Schnitzer, Experimental model of transthoracic, vascular-targeted, photodynamically induced myocardial infarction. *Am. J. Physiol. Heart Circ. Physiol.* **306**, H270–H278 (2014)
- G. Cotter, M. Metra, B.D. Weatherley, H.C. Dittrich, B.M. Massie, P. Ponikowski, D.M. Bloomfield, C.M. O'Connor, Physician-determined worsening heart failure: a novel definition for early worsening heart failure in patients hospitalized for acute heart failure – association with signs and symptoms, hospitalization duration, and 60-day outcomes. *Cardiology* **115**, 29–36 (2010)
- D. Geft, S. Schwartzberg, O. Rogovsky, A. Finkelstein, J. Ablin, S. Mayselauslender, D. Wexler, G. Keren, J. George, Circulating Apoptotic Progenitor Cells in Patients with Congestive Heart Failure. *PLoS One* **3**, 3238 (2008)
- L. Danilowicz-Szymanowicz, J. Suchecka, A. Niemirycz-Makurat, K. Rozwadowska, G. Raczak, Autonomic predictors of hospitalization due to heart failure decompensation in patients with left ventricular systolic dysfunction. *PLoS One* **11**, e0152372 (2016)
- A.M. de Jong, I.C. van Gelder, I. Vreeswijk-Baudoin, M.V. Cannon, W.H. van Gilst, A.H. Maass, Atrial remodeling is directly related to end-diastolic left ventricular pressure in a mouse model of ventricular pressure overload. *PLoS One* **8**, 633–641 (2013)
- P. Donndorf, G. Kundt, A. Kaminski, C. Yerebakan, A. Liebold, G. Steinhoff, A. Glass, Intramyocardial bone marrow stem cell transplantation during coronary artery bypass surgery: a meta-analysis. *J. Thorac. Cardiovasc. Surg.* **142**, 911 (2011)
- V.M. Dragojevic-Simic, S.L. Dobric, D.R. Bokonic, Z.M. Vucinic, S.M. Sinovec, V.M. Jacevic, N.P. Dogovic, Amifostine protection against doxorubicin cardiotoxicity in rats. *Anti-Cancer Drugs* **15**, 169–178 (2004)
- S.M. Eleawa, M. Alkhateeb, S. Ghosh, F. Alhashem, A.S. Shatoor, A. Alhejaily, M.A. Khalil, Coenzyme Q10 protects against acute consequences of experimental myocardial infarction in rats. *Int. J. Physiol Pathophysiol. Pharmacol.* **7**, 1–13 (2015)

- R. Fazan Jr., C.A. Silva, J.A. Oliveira, H.C. Salgado, N. Montano, N. Garcia-Cairasco, Evaluation of cardiovascular risk factors in the Wistar Audiogenic Rat (WAR) Strain. *PLoS One* **10**, e0129574 (2015)
- I. Fernandez-Ruiz, Stem cells: cell therapy improves outcomes in heart failure. *Nat. Rev. Cardiol.* **13**(6), 311 (2016)
- S.A. Fisher, C. Doree, S.J. Brunskill, A. Mathur, E. Martin-Rendon, Bone marrow stem cell treatment for ischemic heart disease in patients with no option of revascularization: a systematic review and meta-analysis. *PLoS One* **8**, e64669 (2013)
- G.S. Francis, Extracardiac features of heart failure: catecholamines and hormonal changes. *Cardiology* **75**(suppl 1), 19–29 (1988)
- R.K. Ghanta, A. Rangaraj, R. Umakanthan, L. Lee, R.G. Laurence, J.A. Fox, R.M. Bolman III, L.H. Cohn, F.Y. Chen, Adjustable, physiological ventricular restraint improves left ventricular mechanics and reduces dilatation in an ovine model of chronic heart failure. *Circulation* **115**, 1201–1210 (2007)
- L. Gullestad, T. Ueland, L.E. Vinge, A. Finsen, A. Yndestad, P. Aukrust, Inflammatory cytokines in heart failure: mediators and markers. *Cardiology* **122**, 23–35 (2012)
- O. Ishida, I. Hagino, N. Nagaya, T. Shimizu, T. Okano, Y. Sawa, H. Mori, T. Yagihara, Adipose-derived stem cell sheet transplantation therapy in a porcine model of chronic heart failure. *Transl. Res.* **165**, 631–639 (2015)
- H. Jaganathan, B. Godin, Biocompatibility assessment of Si-based nano- and micro-particles. *Adv. Drug Deliv. Rev.* **64**, 1800–1819 (2012)
- V. Jeevanantham, M. Butler, A. Saad, A. Abdel-Latif, E.K. Zuba-Surma, B. Dawn, Adult bone marrow cell therapy improves survival and induces long-term improvement in cardiac parameters: a systematic review and meta-analysis. *Circulation* **126**, 551–568 (2012)
- P. Karlström, P. Johansson, U. Dahlström, K. Boman, U. Alehagen, Can BNP-guided therapy improve health-related quality of life, and do responders to BNP-guided heart failure treatment have improved health-related quality of life? Results from the UPSTEP study. *BMC Cardiovasc. Disord.* **16**, 1–10 (2016)
- T. Kawasaki, C. Sakai, K. Harimoto, M. Yamano, S. Miki, T. Kamitani, H. Sugihara, Holter monitoring and long-term prognosis in hypertrophic cardiomyopathy. *Cardiology* **122**, 44–54 (2012)
- N.K. Khan, K.M. Goode, J.G. Cleland, A.S. Rigby, N. Freemantle, J. Eastaugh, A.L. Clark, R. de Silva, M.J. Calvert, K. Swedberg, M. Komajda, V. Mareev, F. Follath, Prevalence of ECG abnormalities in an international survey of patients with suspected or confirmed heart failure at death or discharge. *Eur. J. Heart Fail.* **9**, 491–501 (2007)
- P. Konopelski, M. Ufnal, Electrocardiography in rats: a comparison to human. *Physiol. Res.* **65**, 717–725 (2016)
- K.J. Koomalsingh, W.R. Witschey, J.R. Mcgarvey, T. Shuto, N. Kondo, C. Xu, B.M. Jackson, J.H. Gorman 3rd, R.C. Gorman, J.J. Pilla, Optimized local infarct restraint improves left ventricular function and limits remodeling. *Ann. Thorac. Surg.* **95**, 155–162 (2013)
- Y. Kubota, S. Miyagawa, S. Fukushima, A. Saito, H. Watabe, T. Daimon, Y. Sakai, T. Akita, Y. Sawa, Impact of cardiac support device combined with slow-release prostacyclin agonist in a canine ischemic cardiomyopathy model. *J. Thorac. Cardiovasc. Surg.* **147**, 1081–1087 (2014)
- K.J. Lavine, M. Sintek, E. Novak, G. Ewald, E. Geltman, S. Joseph, J. Pfeifer, D.L. Mann, Coronary collaterals predict improved survival and allograft function in patients with coronary allograft vasculopathy. *J. Heart Lung Transplant.* **32**, S27–S27 (2013)
- J. Li, S. Umar, M. Amjadi, A. Iorga, S. Sharma, R.D. Nadadur, V. Regitz-Zagrosek, M. Eghbali, New frontiers in heart hypertrophy during pregnancy. *Am. J. Cardiovasc. Dis.* **2**, 192–207 (2012)
- F. Limana, M.C. Capogrossi, A. Germani, The epicardium in cardiac repair: from the stem cell view. *Pharmacol. Ther.* **129**, 82–96 (2011)
- S.I. Lok, N. de Jonge, J. van Kuik, A.J. van Geffen, M.M. Huijbers, P. van der Weide, E. Siera, B. Winkens, P.A. Doevendans, R.A. de Weger, P.A. da Costa Martins, MicroRNA expression in myocardial tissue and plasma of patients with end-stage heart failure during LVAD support: comparison of continuous and pulsatile devices. *PLoS One* **10**, e0136404 (2015)
- J.A. Magovern, Experimental and clinical studies with the Paracor cardiac restraint device. *Semin. Thorac. Cardiovasc. Surg.* **17**, 364–368 (2005)
- M. Malatesta, Histological and histochemical methods-theory and practice. *Eur. J. Histochem.* **60**, 2639 (2016)
- R.E. Michler, Stem cell therapy for heart failure. *Cardiol. Rev.* **22**, 105–116 (2014)
- O. Miro, F.W. Peacock, J.J. McMurray, H. Bueno, M. Christ, A.S. Maisel, L. Cullen, M.R. Cowie, S. Di Somma, F.J. Martin Sanchez, E. Platz, J. Masip, U. Zeymer, C. Vrints, S. Price, A. Mebazaa, C. Mueller European society of cardiology-acute cardiovascular care association position paper on safe discharge of acute heart failure patients from the emergency department. *Eur. Heart J. Acute Cardiovasc. Care* **6**(4), 311 (2016)
- M. Naveed, I.S. Mohammad, L. Xue, S. Khan, W. Gang, Y. Cao, Y. Cheng, X. Cui, C. Dingding, Y. Feng, W. Zhijie, Z. Xiaohui, The promising future of ventricular restraint therapy for the management of end-stage heart failure. *Biomed Pharmacother* **99**, 25–32 (2018)
- M. Naveed, L. Wenhua, W. Gang, I.S. Mohammad, M. Abbas, X. Liao, M. Yang, L. Zhang, X. Liu, X. Qi, Y. Chen, L. Jiadi, L. Ye, W. Zhijie, C.D. Ding, Y. Feng, Z. Xiaohui, A novel ventricular restraint device (ASD) repetitively deliver *Salvia miltiorrhiza* to epicardium have good curative effects in heart failure management. *Biomed Pharmacother* **95**, 701–710 (2017)
- G.H. Oliveira, S.G. Al-Kindi, H.G. Bezerra, M.A. Costa, Left ventricular restoration devices. *J. Cardiovasc. Transl. Res.* **7**, 282–291 (2014)
- A.M. Orogo, Å.B. Gustafsson, Cell death in the myocardium: my heart won't go on. *IUBMB Life* **65**, 651–656 (2013)
- Q. Qiu, C. Li, Y. Wang, C. Xiao, Y. Li, Y. Lin, W. Wang, Plasma metabolomics study on Chinese medicine syndrome evolution of heart failure rats caused by LAD ligation. *BMC Complement. Altern. Med.* **14**, 232 (2014)
- T.L. Rasmussen, G. Raveendran, J. Zhang, D.J. Garry, Getting to the heart of myocardial stem cells and cell therapy. *Circulation* **123**, 1771–1779 (2011)
- C. Rüder, T. Haase, A. Krost, N. Langwieser, J. Peter, S. Kamann, D. Zohlhüfer, Combinatorial G-CSF/AMD3100 treatment in cardiac repair after myocardial infarction. *PLoS One* **9**, e104644 (2014)
- S.K. Sanganalmath, R. Bolli, Cell therapy for heart failure: a comprehensive overview of experimental and clinical studies, current challenges, and future directions. *Circ. Res.* **113**(2), 810 (2013)
- S.K. Sanganalmath, R. Bolli, Cell therapy for heart failure: a comprehensive overview of experimental and clinical studies, current challenges, and future directions. *Circ. Res.* **113**(6), 810 (2013).
- A. Shafy, T. Fink, V. Zachar, N. Lila, A. Carpentier, J.C. Chachques, Development of cardiac support bioprostheses for ventricular restoration and myocardial regeneration. *Eur. J. Cardiothorac. Surg.* **43**, 1211–1219 (2013)
- C.C. Sheng, L. Zhou, J. Hao, Current stem cell delivery methods for myocardial repair. *Biomed. Res. Int.* **2013**, 547902 (2013)
- R.R. Smith, E. Marbán, L. Marbán, Enhancing retention and efficacy of cardiosphere-derived cells administered after myocardial infarction using a hyaluronan-gelatin hydrogel. *Biomater* **3**, e24490 (2013)
- R.C. Starling, M. Jessup, Worldwide clinical experience with the CorCap™ cardiac support device. *J. Card. Fail.* **10**, S225–S233 (2004)
- M.M. Sung, J.R. Dyck, Therapeutic potential of resveratrol in heart failure. *Ann. N. Y. Acad. Sci.* **1348**, 32–45 (2015)
- D.A. Taylor, M.J. Robertson, Cardiovascular translational medicine (IX) the basics of cell therapy to treat cardiovascular disease: one cell does not fit all. *Rev. Esp. Cardiol.* **62**, 1032 (2009)

- X. Tian, J. Fan, M. Yu, Y. Zhao, Y. Fang, S. Bai, W. Hou, H. Tong, Adipose stem cells promote smooth Muscle cells to secrete elastin in rat abdominal aortic aneurysm. *PLoS One* **9**, e108105 (2014)
- J.G. Travers, F.A. Kamal, J. Robbins, K.E. Yutzey, B.C. Blaxall, Cardiac fibrosis. Fibroblast Awakens **118**, 1021–1040 (2016)
- B. Vrtovec, G. Poglajen, F. Haddad, Stem cell therapy in patients with heart failure. *Methodist Debaque Cardiovasc. J.* **9**, 6 (2013)
- J.F. Wenk, L. Ge, Z. Zhang, D. Mojsejenko, D.D. Potter, E.E. Tseng, J.M. Guccione, M.B. Ratcliffe, Biventricular finite element modeling of the Acorn CorCap Cardiac Support Device on a failing heart. *Ann. Thorac. Surg.* **95**, 2022–2027 (2013)
- C.W. Yancy, M. Jessup, B. Bozkurt, J. Butler, D.E. Casey, M.H. Drazner, G.C. Fonarow, S.A. Geraci, T. Horwich, J.L. Januzzi, M.R. Johnson, E.K. Kasper, W.C. Levy, F.A. Masoudi, P.E. McBride, J.J.V. McMurray, J.E. Mitchell, P.N. Peterson, B. Riegel, F. Sam, L.W. Stevenson, W.H.W. Tang, E.J. Tsai, B.L. Wilkoff, 2013 ACCF/AHA Guideline for the management of heart failure. *J. Am. Coll. Cardiol.* **62**, e147–e239 (2013)
- J. Yu, M. Li, Z. Qu, D. Yan, D. Li, Q. Ruan, SDF-1/CXCR4-mediated migration of transplanted bone marrow stromal cells toward areas of heart myocardial infarction through activation of PI3K/Akt. *J. Cardiovasc. Pharmacol.* **55**, 496–505 (2010)
- X. Zhou, Active Hydraulic Ventricular Attaching Support System. US. (2012)